Available online at www.sciencedirect.com

SCIENCE DIRECT®

Talanta 64 (2004) 1169–1174

Talanta

www.elsevier.com/locate/talanta

Determination of acid dissociation constants based on continuous titration by feedback-based flow ratiometry

Hideji Tanaka [a,*], Takahiro Tachibana [a], Risa Oda [a], Purnendu K. Dasgupta [b]

[a] *Faculty of Pharmaceutical Sciences, Tokushima University, Shomachi 1-78-1, Tokushima 770-8505, Japan*
[b] *Department of Chemistry and Biochemistry, Texas Tech University, Lubbock, TX 79409-1061, USA*

Received 23 February 2004; received in revised form 13 April 2004; accepted 13 April 2004
Available online 1 June 2004

Abstract

We propose a method for the determination of acid dissociation constants based on the rapid detection of the equivalence point (EP) by feedback-based flow ratiometry and the subsequent estimation of the half equivalence point ($EP_{1/2}$). The titrant (e.g., NaOH) flow rate F_B was varied in response to a control voltage V_c from a controller, while the titrand (e.g., CH_3COOH) flow rate F_A was held constant. The pH of the mixed solution was monitored downstream from the confluence point of the solutions following a knotted tubular mixer. Initially, V_c was increased linearly. At the instance the detector sensed EP, the ramp direction of V_c changed downward. The pH increased further because of the lag time between the mixing of solutions and the sensing of pH. Following the pH maximum, the pH decreased. The EP was sensed again in this downward scan. The V_c that gives $EP_{1/2}$ was computed from the V_c just at the time of the EP detection. The V_c was held constant at this level for 18 s, and the plateau pH value thus obtained was taken to be the pK_a of the analyte subject to activity corrections. Studies on the dependence of the pK_a on the ionic strength or dielectric constant of the solution were conducted in an automated fashion by delivering NaCl solution or acetonitrile through an additional channel. Satisfactory results were obtained with good throughput (53 s per determination) and precision (R.S.D. ≈ 0.3%) for various acids.

Keywords: Flow ratiometry; Flow titration; Feedback-based control; Dissociation constant; Acidity constant

1. Introduction

Flow ratiometry, originated with Blaedel and Laessig [1,2], is a special class of continuous flow analysis, where two independently delivered solutions (e.g., titrand and titrant) are merged at various flow ratios R_f. Analytical signal V_d is monitored at a position downstream of the confluence point of the solutions. The information of interest is determined by analyzing the relationship between R_f and V_d. We have applied the method to continuous on-line titrations [3–5]. The scan range of R_f was limited to a domain just around the equivalence point (EP) by feedback-based control, to realize extremely high throughput titrations (e.g., 3 s per titration [3]). In other related work on the determination of distribution coefficients K_D of an analyte between two phases [6,7], the flow ratio of organic/aqueous flow streams was changed stepwise in order to produce steady analytical signals corresponding to each flow ratio. The throughput of such measurements has recently been improved to 5 min per determination by detecting both phases on-line without phase separation [8].

The acid dissociation constant K_a is just as important as K_D for predicting and explaining the physicochemical and/or biological functions. Generally, an unionized molecule is more lipid soluble and thus penetrates more readily through biological membranes. In such a system, microscopic conditions around the molecules may easily vary and affect the K_a. Fast methods of K_a determination in which the matrix can be readily varied are therefore particularly important to understand the behavior of molecules in complex biological/environmental matrices. Several studies utilizing the paradigms of flow injection analysis (FIA) [9–13] and related techniques [14,15] have been carried out for this purpose; this was discussed elsewhere [16]. More recently, Box et al. [17] reported the K_a for 71 drugs based on a continuous flow scheme with a photodiode array detector. In their

---

[*] Corresponding author. Tel.: +81-88-633-7258; fax: +81-88-633-9508.
E-mail address: htanaka@ph.tokushima-u.ac.jp (H. Tanaka).

0039-9140/$ – see front matter © 2004 Elsevier B.V. All rights reserved.
doi:10.1016/j.talanta.2004.04.007

study, the sample flow was merged with a buffer of temporally changing pH created by mixing "linear buffer" solutions [18] respectively with added HCl and KOH, at different ratios as a function of time. A linear buffer based system for creating a pH gradient using a FIA system was introduced much earlier [9].

In our previous paper [16], feedback-based flow ratiometry was used for the rapid determination of K_a. In this approach, titrant (NaOH) flow rate was varied with the total (titrant + titrand) flow rate maintained constant. The half equivalence point ($EP_{1/2}$) was directly determined by rapid upward and downward scans of titrant/titrand flow ratio. The method was applied to low molecular *n*-alkyl carboxylic acids (C = 1–5) and H_3PO_4. High throughput (ca. 26 s per determination) was attainable with reasonable precision (relative standard deviation (R.S.D.) ≈ 3%). The method was, however, susceptible to detector noise, although the bias in pK_a caused by the noise did not seem to be significant. Nevertheless, extensive noise filtration is required to improve reliability and this is incompatible with high throughput [19]. The determination of EP is less affected by noise [3–5] because the pH jump around EP is large compared to the noise. In the present study, we therefore explored an alternative approach for K_a determination through the detection of EP by feedback-based flow ratiometry and the succeeding estimation of $EP_{1/2}$. Compared to the previous approach [16], the presently proposed method needs a little longer time (53 s per determination), but the precision is improved by an order of magnitude (R.S.D. ≈ 0.3%).

2. Experimental

2.1. Flow system

Fig. 1 shows the flow system. Two peristaltic pumps (P_1 and P_2; Rainin Dynamax RP-1) were used for delivering titrand (A) and titrant (B), respectively. Both solutions were continuously helium-degassed in order to prevent the influence of CO_2 from ambient air. The experimental environment was air-conditioned at 25 °C, but beyond this the experimental temperature was not controlled. The pump tubes used were 0.51 mm i.d. Pharmed® tubing. The flow rate F_A of a titrand was held constant at 0.50 $cm^3\,min^{-1}$. The flow rate F_B of a titrant (0.1 $mol\,dm^{-3}$ NaOH or HCl) varied in response to a control voltage V_c (0–5 V) generated from an algorithm-based controller (PC; Toshiba Dynabook Satellite 1800 SA95C/4 notebook computer) through a PC card (Measurement Computing PC-CARD-DAS16/12-AO). Code written in Visual BASIC® in-house was used to generate V_c, acquire data, analyze them and graphically display the results. The titrant and titrand were merged in a polypropylene-tee and led to a mixing reactor (MR: 0.5 mm i.d., 50 cm long PTFE (Teflon) knotted tubing). The mixed solution was allowed to come into a flow cell (FC; Horiba 6941-15C flow-through glass electrode) equipped with a reference electrode (Horiba 2461A-15T), both the electrodes being connected to a Horiba F-13 pH meter (D). The electrode was calibrated daily before the measurements with commercial standard pH buffers in flow mode. Output signal (V_d) from the pH meter (−0.7 to +0.7 V for pH 0–14) was digitized by the PC card at the frequency of 10 Hz and the resulting data were directly acquired in the Microsoft Excel® format.

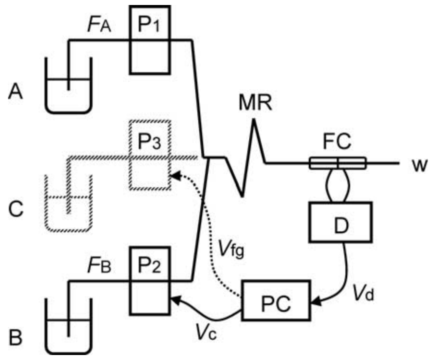

Fig. 1. Flow diagram of a flow ratiometry system. (A) Titrand (typically 0.1 $mol\,dm^{-3}$ acid); (B) titrant (typically 0.1 $mol\,dm^{-3}$ NaOH); (C) additive (2 $mol\,dm^{-3}$ NaCl or acetonitrile); W, waste; P_1–P_3, peristaltic pump; MR, mixing reactor; FC, flow cell (flow-through glass electrode equipped with a reference electrode); (D) pH meter; PC, controller (notebook computer). F_A and F_B are the flow rates of titrant and titrate, respectively. V_c and V_{fg} are the controller output voltages for titrant and additive flow rates, respectively. V_d is the detector output. For the pK_a determination in the presence of NaCl or acetonitrile, the third channel shown by the broken lines was added to the system.

In some experiments, the third channel shown by the broken lines in Fig. 1 was used for automatically changing the ionic strength or the dielectric constant (permittivity). Sodium chloride (2 $mol\,dm^{-3}$) or acetonitrile was delivered by using the third pump (P_3: the same model as P_1 and P_2). The pump speed of P_3 could also be varied automatically by using another controller output voltage (V_{fg}) from the controller.

2.2. Reagents

Reagents (analytical reagent grade; Kanto Chemicals or Nacalai Tesque) were used without further purification. Milli-Q SP grade deionized water was used throughout.

3. Principles

Fig. 2 illustrates the principle of the present method by using real data for the titration of 0.1 $mol\,dm^{-3}$ CH_3COOH with 0.1 $mol\,dm^{-3}$ NaOH. Initially, the controller output voltage V_c, and thus the NaOH flow rate F_B increases linearly. The value of V_c determines the composition of the mixed solution at the confluence point of both the solutions. The pH of the mixed solution being detected increases after a delay. This delay is primarily determined by the physi-

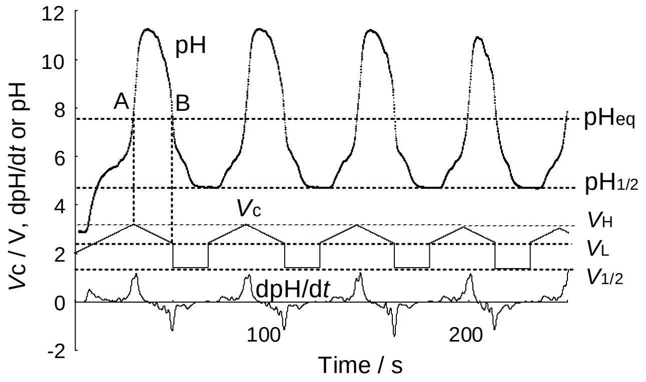

Fig. 2. The principle of feedback-based flow ratiometry for pK_a determination based on rapid detection of equivalence point. Titrand: 0.1 mol dm^{-3} CH_3COOH; titrant: 0.1 mol dm^{-3} NaOH. The meaning of each symbol is described in the text.

cal transit time of the merged solutions from the confluence point to the flow cell and to a lesser extent by the electrode response time. In the present configuration, the physical transit time is not constant but is dependent on V_c. At the instant the detector senses EP (A), where the slope of the titration curve (dpH/dt) becomes maximum, the ramp direction of V_c is changed downwards. The value of V_c at this inflection point thus constitutes V_H. The pH of the mixed solution continues to increase because of the lag time, and then decreases after reaching a maximum. The EP is sensed again (B) in the course of this downward scan. The value of V_c at this point constitutes V_L. The value of V_c that gives the composition corresponding to EP at the confluence point (V_{eq}) can be estimated from the V_H and V_L values by assuming that the electrode response time is negligible in comparison with the physical transit time. If the total (titrand + titrant) flow rate were constant as in the previous system [16], the V_{eq} value could be easily calculated by averaging the values of V_H and V_L. In the present system, however, the total flow rate is not constant but depends on V_c. The delay from V_{eq} to V_H in the upward scan is shorter than that from V_{eq} to V_L in the downward scan. This fact makes the computing of the V_{eq} value a little more complicated. Consider that the transit volume between the mixing point and the detector is R. The total flow rate at any time is ($F_A + F_B$) where the variable flow rate F_B is linearly related to the control voltage V_c as

$$F_B = kV_c \tag{1}$$

During the transition between V_{eq} and V_H, time t_H elapses and the mean F_B flow rate experienced by the residence volume in this period is given by $k(V_{eq} + V_H)/2$ and thus, based on the total flow rate $F_A + F_B$

$$t_H = \frac{R}{\{F_A + 0.5k(V_{eq} + V_H)\}} \tag{2}$$

If the ramp rate (dV_c/dt) of the chosen waveform is expressed as r, it also follows that

$$V_H = V_{eq} + rt_H \tag{3}$$

and therefore

$$t_H = \frac{(V_H - V_{eq})}{r} \tag{4}$$

Eqs. (2) and (4) lead to

$$(V_H - V_{eq})\{F_A + 0.5k(V_{eq} + V_H)\} = rR \tag{5}$$

similarly going from V_{eq} to V_L on the downramp takes time t_L

$$t_L = \frac{R}{\{F_A + 0.5k(V_{eq} + V_L)\}} = \frac{(V_{eq} - V_L)}{r} \tag{6}$$

Hence, from Eq. (6)

$$(V_{eq} - V_L)\{F_A + 0.5k(V_{eq} + V_L)\} = rR \tag{7}$$

Equating, Eqs. (5) and (7)

$$\begin{aligned}(V_H - V_{eq})\{F_A + 0.5k(V_{eq} + V_H)\} &= (V_{eq} - V_L)\\ &\quad \{F_A + 0.5k(V_{eq} + V_L)\}\end{aligned} \tag{8}$$

that simplifies to

$$\begin{aligned}V_{eq}^2 + \left(2\frac{F_A}{k}\right)V_{eq} - \left(\frac{F_A}{k}\right)(V_H + V_L)\\ -0.5(V_H^2 + V_L^2) = 0\end{aligned} \tag{9}$$

The applicable solution to this quadratic equation is

$$V_{eq} = -\frac{F_A}{k} + \sqrt{\frac{{F_A}^2}{k^2} + \frac{V_H^2 + V_L^2}{2} + \frac{F_A(V_H + V_L)}{k}} \tag{10}$$

One of the merits of the present flow mode with a constant titrand flow rate is that the V_c that gives the half equivalence point ($V_{1/2}$) can be estimated easily from V_{eq}. For example, for monoprotic acid, $V_{1/2}$ equals to $0.5V_{eq}$. For diprotic acids, $V_{1/2}$ equals to $0.5V_{eq1}$ and $0.75V_{eq2}$ for the pK_{a1} and pK_{a2} determinations, respectively. At the $V_{1/2}$ level, V_c is held constant for 18 s, where the first 15 s constitutes the waiting period to ensure that a stable pH signal ($pH_{1/2}$) corresponding to $V_{1/2}$, has been reached and the next 3 s is then devoted to signal integration and data acquisition. This way, better reproducibility for the determination of pK_a is obtained; the pK_a of the analyte under the test conditions is determined from the mean of $pH_{1/2}$ over the 3 s period (to which activity correction is then applied). For example, for monoprotic acids of H^+A^- (e.g., CH_3COOH) and BH^+ (e.g., ${NH_4}^+$), the pK_a values were calculated from the equations $pK_a = pH_{1/2} - \log\gamma_{A-}$ and $pK_a = pH_{1/2} + \log\gamma_{BH+}$, respectively; for diprotic acid $(H^+)_2A^{2-}$ (e.g., H_2CO_3), $pK_{a1} = pH_{1/2} - \log\gamma_{HA-}$, and $pK_{a2} = pH_{1/2} - \log\gamma_{A2-} + \log\gamma_{HA-}$, where γ is the activity coefficient of the subscript ion. Activity coefficient of the ion is calculated according to the Davies equation [20]

$$\log\gamma_i = -0.51z_i^2\left(\frac{\sqrt{I}}{1+\sqrt{I}} - 0.3I\right) \tag{11}$$

where z_i is the charge magnitude of the ion and I is the ionic strength of the medium.

4. Results and discussion

4.1. System set-up

The scan rate of V_c was investigated in the range of 5–100 mV s^{-1} by using 0.1 mol dm^{-3} CH_3COOH and 0.1 mol dm^{-3} NaOH as titrand and titrant, respectively. The pK_a values obtained are plotted as a function of the scan rate in Fig. 3 along with ±1 standard deviation depicted as the error bar. While the effect of scan rate on the mean pK_a value obtained was insignificant, it obviously had large effect on the precision of the measurement. The rate of pH change increases as the scan rate (and hence the titrand flow rate) increases. Operationally, this made it more difficult to locate EP precisely at high scan rates, resulting in large uncertainties at scan rates >60 mV s^{-1}. Scans rates $\geq$ 90 mV s^{-1} sometimes failed to find EP altogether because, depending on the pK_a, the titrand concentration and the presence of the finite transit time, V_c may reach its scan limit (0 or 5 V) before EP is detected. On the other hand, scan rates of $\leq$10 mV s^{-1} also failed to find EP because the slope of the titration curve decreased sufficiently to render the detection of EP more susceptible to detector noise. The effect of the scan rate was further investigated at 30, 40 and 50 mV s^{-1} by applying the method to several *n*-alkyl carboxylic acids (C = 1, 3–5) and H_3PO_4. The best results were obtained at the scan rate of 40 mV s^{-1} and further work was conducted at this scan rate.

The effects of the nature and the length of the mixing reactor were examined by using knotted tubular reactors (0.5 mm i.d.; 25, 50 or 100 cm long, knot diameter ~0.5 cm) [21] and single bead string reactors (1 mm i.d.; 5, 10 or 20 cm long; 0.6 mm bead diameter). The relative standard deviation (R.S.D.) of pK_a for CH_3COOH was $\leq$0.3 and $\leq$0.6% for the two reactor types, respectively, with no significant effect of the reactor length within the range examined. Further work was therefore conducted with a 50 cm knotted tubular reactor.

Data acquisition frequency and noise filtration techniques were investigated to see if the reliability of the measurement can be improved by varying those parameters. From the results for extensive sets of the experimental tests, we selected 10 Hz as data acquisition frequency. A moving average filter that used 11 consecutive raw V_d values was utilized and the data thus generated was processed a second time through an identical filter.

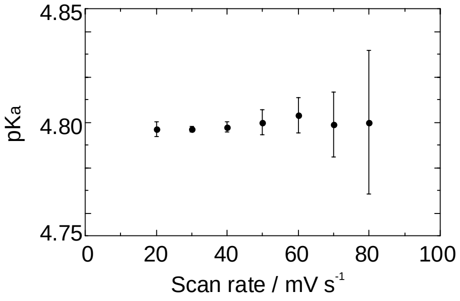

Fig. 3. Effect of scan rate on the pK_a and its standard deviation of CH_3COOH. Titrand and titrant are the same as those in Fig. 2.

In contrast to the previous approach [16], where $EP_{1/2}$ is determined directly, the present approach requires the calibration of flow rates because V_{eq} and thus $V_{1/2}$ are expressed as a function of both F_A and F_B (see Eq. (10)). If the flow rate changed from the calibrated values, this error can affect the estimation of $V_{1/2}$. In order to ascertain the extent of this influence, we intentionally biased F_A or k ($=F_B/V_c$) to slightly erroneous values as software parameters and compared the pK_a of CH_3COOH thus obtained with that determined with the correct values of F_A and k. Errors in F_A ranging from −10, −5, −1, +1, +5 to +10% were found to cause -0.004 ± 0.004, -0.001 ± 0.007, $+0.0003 \pm 0.007$, $+0.0005 \pm 0.014$, -0.006 ± 0.006% and -0.018 ± 0.004 errors in pK_a, respectively. Similar variations in k caused $+0.006\pm0.020$, -0.005 ± 0.015, $+0.005\pm0.007$, $+0.001\pm 0.005$, $+0.009 \pm 0.016$ and $+0.052 \pm 0.006$ errors, respectively (n = 3–5). The maximum bias in pK_a was −0.018 (relative error 0.39%) resulting from a +10% error in F_A. The fact that the buffer capacity of the mixed solution is maximum at $EP_{1/2}$ makes the determined value of pK_a relatively insensitive to the various possible sources of error.

4.2. Applications to various acids and bases

The dissociation constants of various acids and bases as determined by the present method are listed in Table 1 along with the literature values [22–25]. In the case of H_2CO_3 and NH_4^+, their conjugate bases (CO_3^{2-} (taken as Na_2CO_3) and NH_3) were titrated with 0.1 mol dm^{-3} HCl. For H_3PO_4 and H_2CO_3, the first or second dissociation constants were independently determined by presetting the lower and upper pH limits for the EP detection so as to confine the system to the desired titration step. For example, pH 3–6 and 8–12 were the respective set limits for the first and the second titration steps of H_3PO_4. The values obtained by the present automated approach were in good agreement with the literature data. the largest standard deviations was maximally 0.076 for the pK_{a2} of H_3PO_4, amounting to 1.05% in R.S.D.

4.3. Effect of ionic strength or dielectric constant

By using the configurations with three pumps (Fig. 1), NaCl or acetonitrile (MeCN) was delivered at various flow rates. The results for the titration of CH_3COOH with NaOH in the presence of NaCl and MeCN are plotted together in Fig. 4. The V_{fg} (the control voltage for P_3 pump) was increased and then decreased stepwise during the period of 50 min. In this period, the concentrations of NaCl and MeCN at $EP_{1/2}$ level were changed between 0 and 1.14 mol dm^{-3} and between 0 and 40 vol.%, respectively. For pH measurement over a long period, the software was modified to prevent data overflow (>65,536 lines). In this version, the most

Table 1
Dissociation constants of acids determined by flow ratiometry

Analyte		pK_a	S.D. (n)	Literature values[a]
Formic acid (HCOOH)		3.761	0.007 (4)	3.75 [22,23]
Acetic acid (CH_3COOH)		4.784	0.002 (3)	4.756 [22], 4.76 [23]
Propanoic acid (C_2H_5COOH)		4.877	0.001 (4)	4.87 [22,24], 4.88 [23]
n-Butanoic acid (C_3H_7COOH)		4.855	0.007 (8)	4.82 [23], 4.83 [22]
n-Pentanoic acid (C_4H_9COOH)		4.873	0.010 (8)	4.83 a [22]
Phosphoric acid (H_3PO_4)	pK_{a1}	2.095	0.012 (4)	2.15 [25], 2.16 [22]
	pK_{a2}	7.206	0.008 (4)	7.20 [25], 7.21 [22]
Ammonium ion (NH_4^+)		9.287	0.003 (6)	9.25 [22]
Carbonic acid (H_2CO_3)	pK_{a1}	6.313	0.021 (9)	6.35 [22]
	pK_{a2}	10.611	0.019 (9)	10.33 [22]

[a] At 25 °C except for the value denoted by the letter “a” (20 °C).

recent 1000 data points for V_c, pH and dpH/dt were collected and displayed as in Fig. 2, whereas V_{fg} (5 s resolution) and the value of $pH_{1/2}$ at $EP_{1/2}$ are collected and displayed over the whole measurement period (Fig. 4). Similar experiments were carried out for the titration of NH_3 with HCl in the ranges of NaCl and MeCN concentrations 0–0.57 mol dm^{-3} and 0–40 vol.%, respectively.

The pK_a values of CH_3COOH and NH_4^+ measured as a function of ionic strength (that contributed by CH_3COO^-, H^+, NH_4^+ and OH^- at $EP_{1/2}$ was also included) in the presence of NaCl are shown as the closed circles and triangles, respectively, in Fig. 5A. The two open symbols are the respective literature values [22]. The results seem reasonable because the determined values of pK_a with activity correction are almost constant irrespective of the ionic strength.

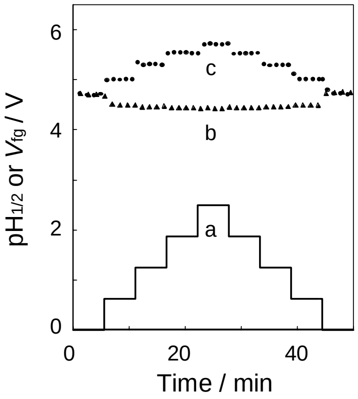

Fig. 4. The pK_a determination of CH_3COOH in matrices of changing composition. (a) V_{fg}; (b and c) pH at the half equivalence point in the presence of NaCl and acetonitrile, respectively.

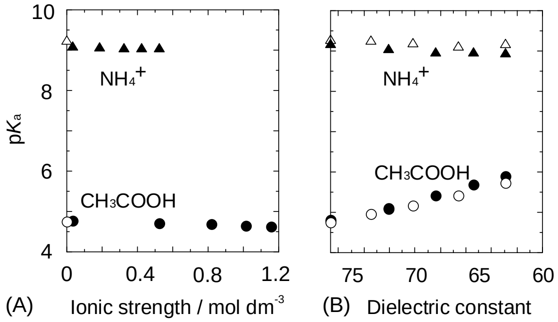

Fig. 5. Effect of ionic strength (A) and dielectric constant (B) on the pK_a of CH_3COOH and NH_4^+. Closed and open symbols are the experimental and literature values of pK_a.

For the measurement of pH in a mixed solvent, the electrode should be calibrated with standard pH buffers in the same solvent as samples. Such a procedure can be implemented in the present system but at the expense of considerable complexity. Presently, the pH in mixed solvent (${}^{s}_{w}$pH) was measured by using an electrode pre-calibrated with aqueous standard buffers. Then, this ${}^{s}_{w}$pH was corrected by taking into account the mole fraction of MeCN, X_{MeCN}, by the experimentally obtained equation following the recommendations in [26]:

$${}^{s}_{s}\mathrm{pH} = {}^{s}_{w}\mathrm{pH} + 3.81X_{\mathrm{MeCN}} \tag{12}$$

where ^{s}spH means the pH in a MeCN–H_2O medium, referred to the standard pH buffers containing MeCN at the same X_{MeCN} as in the sample. Thus corrected ${}^{s}_{s}$pk_a is shown in Fig. 5 by the closed symbols as a function of the dielectric constant. The dielectric constant (ε of the MeCN–H_2O media were estimated from the Eq. (13) [26].

$$\varepsilon^{-1} = 0.01547X_{\mathrm{MeCN}} + 0.01305 \tag{13}$$

The values obtained in the present experiments (Fig. 5B) agreed well with the literature values [26,27] (shown as open symbols); the pK_a values for CH_3COOH (closed circles) increased with decreasing ε and those for NH_4^+ (closed triangles) were almost constant irrespective of ε. From these results, we concluded that the present system is capable of accurately determining pK_a in matrices of high ionic strength and lower dielectric constant, at least within the realm of the experiments presently conducted.

5. Conclusion

We have applied feedback-based flow ratiometry for the determination of acidity constants based on the rapid determination of the equivalence point (EP) and the subsequent measurement of the half equivalence point ($EP_{1/2}$). The present method can be determines a pK_a value with high precision ($\leq$0.3% R.S.D.) in under 1 min, thus making it useful for rapid estimation of K_a for a variety of compounds in varying matrices.

References

[1] W.J. Blaedel, R.H. Laessig, Anal. Chem. 36 (1964) 1617.
[2] W.J. Blaedel, R.H. Laessig, Anal. Chem. 37 (1965) 332.
[3] H. Tanaka, P.K. Dasgupta, J. Huang, Anal. Chem. 72 (2000) 4713.
[4] P.K. Dasgupta, H. Tanaka, K.D. Jo, Anal. Chim. Acta 435 (2001) 289.
[5] K.D. Jo, P.K. Dasgupta, Talanta 60 (2003) 131.
[6] H. Tanaka, T. Tachibana, H. Chuman, Anal. Sci. 17 (2001) i1403.
[7] H. Tanaka, T. Tachibana, K. Aritsuka, H. Chuman, J. Flow Inject. Anal. 20 (2003) 43.
[8] H. Tanaka, Bunseki Kagaku 53 (2004) 359.
[9] R.S. Vithanage, P.K. Dasgupta, Anal. Chem. 58 (1986) 326.
[10] D.R. Turner, S. Knox, M. Whithield, M.D. Santos, C. Pescada, M.D.L. Gonçalves Lurdes, Anal. Chim. Acta 226 (1989) 229.
[11] M. Agudo, J. Macros, A. Ríos, M. Valcárcel, Anal. Chim. Acta 239 (1990) 211.
[12] L. Nørgaard, Anal. Chim. Acta 255 (1991) 143.
[13] J. Saurina, S. Hernández-Cassou, R. Tauler, A. Izquierdo-Ridorsa, Anal. Chim. Acta 408 (2000) 135.
[14] J. Marcos, A. Ríos, M. Valcárcel, Anal. Chem. 62 (1990) 2237.
[15] K. Carlsson, B. Karlberg, Anal. Chim. Acta 434 (2001) 149.
[16] H. Tanaka, K. Aritsuka, T. Tachibana, H. Chuman, P.K. Dasgupta, Anal. Chim. Acta 499 (2003) 199.
[17] K. Box, C. Bevan, J. Comer, A. Hill, R. Allen, D. Reynolds, Anal. Chem. 75 (2003) 883.
[18] O. Åstrom, Anal. Chim. Acta 88 (1977) 17.
[19] H. Tanaka, T. Tachibana, Anal. Sci., in press.
[20] G.D. Christian, Analytical Chemistry, sixth ed., Wiley, New York, 2004, p. 213.
[21] S. Waiz, B.M. Cedillo, S. Jambunathan, S.G. Hohnholt, P.K. Dasgupta, D.K. Wolcott, Anal. Chim. Acta 428 (2001) 163.
[22] D.R. Lide (Ed.-in-chief), CRC Handbook of Chemistry and Physics, 84th ed., CRC Press, Boca Raton, 2003, pp. 8-46–8-51.
[23] P.H. Howard, W.M. Meyhan (Eds.), Handbook of Physical Properties of Organic Chemicals, CRC Press, Boca Raton, 1997.
[24] The Merck Index, 13th ed., Merck & Co., Whitehouse Station, 2001.
[25] The Chemical Society of Japan (Ed.), Kagaku Binran, Kiso-hen, Handbook of Chemistry, third ed., Maruzen, Tokyo, 1984, pp. II 338–342 (in Japanese).
[26] S. Espinosa, E. Bosch, M. Rosés, Anal. Chem. 72 (2000) 5193.
[27] S. Espinosa, E. Bosch, M. Rosés, J. Chromatogr. A 964 (2002) 55.